Study the Interface Shape of Tooling and Work Piece Contact During a Flow Forming Operation

Hamidreza Gharehchahi and Amin Etminan

***Abstract*—** In the last two decades or so, flow forming has gradually matured as metal forming process for the production of engineering components in small to medium batch quantities. Flow forming technique is being utilized increasingly due to the great flexibility provided for producing complicated parts nearer to net shape, enabling customers to optimize designs and reduce weight and cost, all of which are vital, especially in automotive industries. But this method involves complicated tooling/workpiece interactions. Purely analytical models of the tool contact area are difficult to formulate, resulting in numerical approaches that are case-specific. Provided are the details of an analytical model that describes the steady-state tooling/workpiece contact area allowing for easy modification of the dominant geometric variables. The assumptions made in formulating this analytical model are validated with experimental results attained from physical modeling. The analysis procedure can be extended to other rotary forming operations such as metal spinning, shear forming, thread rolling and crankshaft fillet rolling.

***Keywords*—** Finite element, Flow Forming, Piece Contact

I. INTRODUCTION

TO determine the energy required to form a component, the size and orientation of the tooling interface on the workpiece is necessary. While purely analytical models describing this contact are preferable, they are usually difficult to attain for complex metal forming processes. In this study, an analytical approach is presented to model the tooling/workpiece contact area in an application of rotary forming. While the present work focuses on an implementation for flow forming, the applied technique can be applied to other variants of rotary forming operations such as metal spinning, shear forming, thread rolling and crankshaft fillet rolling. Flow forming, a variant of metal spinning, is a process used to fabricate rotationally symmetrical parts from ductile materials, after Wong etal.(2003). During flow forming, the work piece is clamped to a rotating mandrel and pressed into contact with the mandrel by rollers. The rollers induce high levels of plasticity in the workpiece causing it to undergo both reduction in thickness and axial lengthening. Since the rollers press on only a very small area of the overall workpiece at any given time, the deformation is highly localized between the roller and workpiece. To properly understand the distribution of this intense local plastic deformation it is essential to be able to calculate the roller/workpiece contact area from the geometric parameters that govern the flow forming process. In addition, the roller/workpiece contact area is critical to coupling other experimental findings, such as power consumption, frictional effects, force, stress and strain distributions through the workpiece back to geometric process parameters. In flow forming, the combined mandrel rotation and linear movement of the rollers induce contact on the workpiece along a helical path. This helical tool path, coupled with the curved profile of the rollers leads to a very complicated roller/workpiece contact area. [1-4]

Hamidreza Gharehchahi is with the Department of Mechanical Engineering, Neyriz Branch, Islamic Azad University, Neyriz, Iran. (Phone: +989178341218; fax: +987325230713e-mail: gharehchahi@chmail.ir).

Amin Etminan, is with the Department of Mechanical Engineering, Neyriz Branch, Islamic Azad University, Neyriz, Iran. (Phone: +989177129151; fax: +987325230713; e-mail: etminan.amin@gmail.com).

II. CONTACT SOLUTION

During flow forming, the roller contacts the workpiece along a path having a constant pitch (Fig. 1). The profile of the roller can be divided in to three regions: the entry region, the nose region and the exit region. These regions dictate the size and shape of the roller/workpiece contact area. The contact area is bounded by three contours: the tangential exit contour, the axial entry contour and the axial exit contour, labeled 1–3,respectivelyin Fig. 2(a). The contact area extends angularly from the tangential exit contour ($\theta = 0$) through to $\theta = \theta f$ (Fig. 2(b)). If the roller has an archetypal flow forming profile similar to that shown in Fig. 1 with distinct flat entry and exit regions and a blending radius between the two that creates a nosed roller, the final contact area is dependent on six surfaces(Fig. 3). Contour1 and the starting points of contours 2 and 3 (Fig. 2) can be calculated directly as they lie exclusively on the xz-plane. The a priori z-coordinates of the extents of contour 1 define the axial limits of the roller/workpiece contact area. Once a solution has been found for the starting and ending points of contour1(by definition the starting points of contours 2 and 3),the common end point of contours 2 and 3 is then solved using an iterative technique. [5]

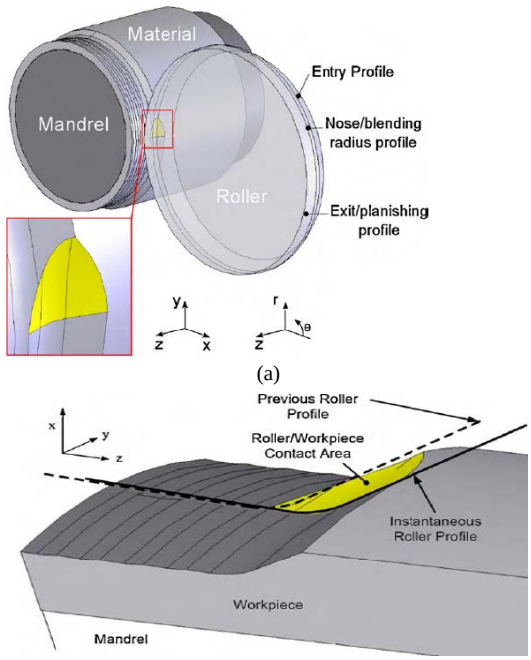

Fig.1. (a) Single roller contact in flow forming showing the mandrel and key roller profiles and (b) Roller profiles deciding the instantaneous contact area during flow forming. There are six in total: the nosed region of the roller from the previous workpiece rotation, the entry region of the roller from the previous workpiece rotation, the instantaneous roller exit region, the instantaneous roller nosed region, the instantaneous roller entry region and the outer surface of the unformed workpiece.

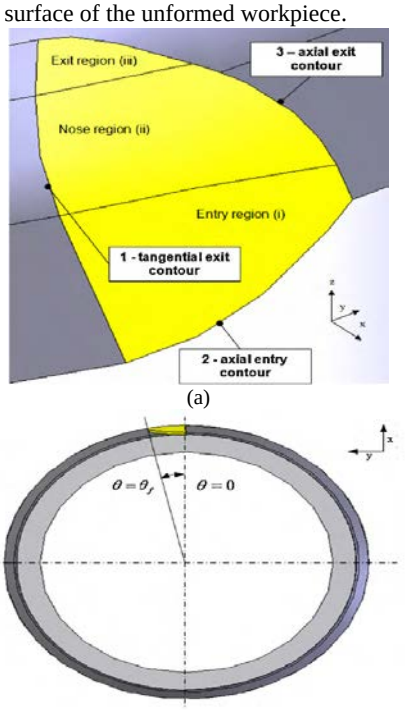

Fig.2. (a) detail of roller contact showing different zones and contour numbers and (b) contact extends angularly from θ to θf

III. AXIAL LIMITS

It is first necessary to calculate the axial limits of contact by determining the end points of contour1. Contour 2 is a function of the instantaneous roller contact with the workpiece at pitch P=0. Contour 3 is a function of the instantaneous roller contact on the material as well as the tool contact on the workpiece one revolution of the mandrel be forehand, at P = fz/n. Contour1exists solely on the xz plane and is bound by the points of intersection with contours 2 and 3.Contour 1 is both dependent on roller geometry and the roller path pitch, P. There are four possible conditions describing the intersection of the current roller position with that of its position on the previous mandrel revolution. Calculation of the location of the upper endpoint of contour 1 for the four conditions shown in Fig. 3 is accomplished through comparison of the endpoints of the roller nose profile on the xz plane. For comparison purposes, the local coordinate system is moved on the x axis from the global origin by d−Rr −R (Fig. 1-b). The x and z coordinates of the upper end point of the nosed region of contour 1, xu and zu (Fig. 3): [5]

$$x_u = R-(1-\cos\beta)\,,\quad z_u = R\sin\beta \tag{1}$$

For the lower x and z coordinates of the endpoint of the nose region of contour1, xl and zl (Fig. 1-b):

$$x_l = R-(1-\cos\alpha)\,,\quad z_l = -R\sin\alpha \tag{2}$$

The entry profile of the previous roller path and the instantaneous exit profile of the roller will occur at xi and zi. These are expressed as:

$$x_i = \frac{R(\sin\alpha\cos\beta+\sin\beta\cos\alpha-\sin\beta-\sin\varepsilon)+P\sin\alpha\sin\beta}{\cos\beta\sin\alpha+\sin\beta\cos\alpha}\,,$$
$$z_i = \frac{R(\cos\alpha-\cos\beta)+P\cos\beta\sin\alpha}{\cos\beta\sin\alpha+\sin\beta\cos\alpha} \tag{3}$$

The values of xu, xl, xi, zu, zl and zi can be compared to identify which contact condition shown in Fig.2 applies. Once the proper contact condition is determined, a solution for the z coordinate for the upper endpoint of contour 1 ,as well as the upper axial limit of the solution space, z1-3, is possible. Solving z1-3 for the appropriate condition A through D.

$$z_{1-3}\{A\} = \frac{P}{2}\,,\quad z_{1-3}\{C\} = \begin{Bmatrix} z = \sqrt{R^2-(x-R)^2} \\ z = \dfrac{x}{\tan\alpha}+\left(\dfrac{x_l}{\tan\alpha}+z_l+P\right)\end{Bmatrix},$$
$$z_{1-3}\{D\} = \begin{Bmatrix} z = P-\sqrt{R^2-(x-R)^2} \\ z = \dfrac{x}{\tan\beta}+z_u-\dfrac{x_u}{\tan\beta}\end{Bmatrix} \tag{4}$$
$$z_{1-3}\{B\} = z_l$$

In conditions C and D, z1-3 is expressed as the solution that satisfies the two equations for z. The lower endpoint of contour 1, z1-2, occurs at the intersection of the profile of the instantaneous roller position and the cylinder with radius Ri. This intersection depends on roller geometry and the depth that it penetrates into the workpiece. Either the roller intersects the workpiece at the flat entry region (condition I) or the nosed region (condition II). If the roller intersects at the flat entry region: [5]

$$x_l \le t_f \tag{5}$$

Otherwise, condition II prevails and the roller intersects within the nosed region. The solution for this intersection point yields the following expressions for the lower endpoint of contour 1 and the lower axial limit of the solution space. This value, z1-2, for each condition is given as:

$$z_{1-2}\{I\} = -\left(\frac{t_0 - t_f + R(\sec\alpha - 1)}{\tan\alpha}\right),$$

$$z_{1-2}\{II\} = -\sqrt{\left(-t_0^2 + 2t_0t_f - t_f^2 + 2Rt_0 - 2Rt_f\right)} \quad (6)$$

Thus far, the region where the tool contact resides has been explicitly bound in the axial direction between z1-3 and z1-2. The following describe show the components needed for a computation of the full three dimensional contact area are developed. These components are the maximum angular limit that the solution space can be defined by and the surfaces that bind the solution space of the instantaneous contact. [5]

IV. Maximum angular limit

Contours corresponding to the ones described in Section 2 that pass through the axial limits, z1-3 and z1-2, are formulated to extend angularly from θ=0 to θ = θmax . This value is the absolute maximum value that can be, corresponding to P≈ 0. The extreme point at angle θmax lies on the xy plane at z = 0; its coordinates are obtained using the same derivation as the general solution for the contact of two circles using the global datum. The first circle is one centered at x, y = 0 with a radius of Ri and the other is at a distance x = d and y = 0 with a radius of Rr + R. [5]

$$\theta_{\max} = \arctan\left(\frac{y_{\max}}{x_{\max}}\right), \quad x_{\max} = \frac{d^2 - (R_r + R)^2 + R_i^2}{2d},$$

$$y_{\max} = \frac{\sqrt{4d^2R_i^2 - (d^2 - (R_r + R)^2 + R_i^2)^2}}{2d} \quad (7)$$

V. Surface definitions

As described in Section 2, there are six different surfaces that define the area. Due to the system complexity, a numerical technique is employed to generate these boundary surfaces in three dimensions. In this technique, the overall solution space is represented by a finite number of points or nodes. For example, if the solution space was broken up into 20×20×20 uniformly spaced points, then the resolution, R*, of the space would be 20. Fig. 6 shows the effect on the solution by increasing or decreasing R*. The following are the definitions of the arrays of coordinates used to define the boundary surfaces as functions of R*, where initially n = R* and decays for every term included in the array until n=1.

$$z_{1\times R^*}(n) = z_u - (R^* - n)\left(\frac{z_u - z_l}{R^* - 1}\right),$$

$$y_{1\times R^*}(n) = (R^* - n)\left(\frac{R_i \sin\theta_f}{R^* - 1}\right), \quad \theta_{1\times R^*}(n) = (R^* - n)\left(\frac{\theta_f}{R^* - 1}\right) \quad (8)$$

Now that the arrays of points are formulated, the boundary surfaces can be formed as m= R* by n = R* square matrices for each direction through space to form Zm,n, Ym,n and θm,n. The m direction of these matrices is a solution for z at a given value in the n direction of y or θ. The following are functions of discrete entries in the matrices that define the boundary surfaces. Starting with the instantaneous roller position: [5-8]

$$x_{i_{m,n}} = \begin{Bmatrix} d + \frac{R(\cos\beta - \cos\alpha)}{\cos\alpha\cos\beta} - (\phi - z_{m,n}\tan\beta)\sqrt{1 - \frac{R_i^2\sin^2\theta_{m,n}}{\phi^2}} \\ d - (\phi - z_{m,n}\tan\beta)\sqrt{1 - \frac{R_i^2\sin^2\theta_{m,n}}{\phi^2}} \\ d - \sqrt{((R^2 - z_{m,n}^2)^{1/2} + R_r^2) - y_{m,n}^2} \end{Bmatrix} \quad (9)$$

Where, φ= Rr + (R/cosα). Zi,m,n and Yi,m,n remain the matrices of dimension R* by R*:

$$y_{i_{m,n}} = y_{m,n}, \quad z_{i_{m,n}} = z_{m,n} \quad (10)$$

The cylindrical surface defined by Ri that describes the outer surface of the workpiece formed around the mandrel:

$$x_{m_{m,n}} = R_i\cos\theta_{m,n}, \quad y_{m_{m,n}} = R_i\sin\theta_{m,n}, \quad z_{m_{m,n}} = z_{i_{m,n}} \quad (11)$$

For the previous roller path, the surfaces are most easily defined in radial expressions, and translated to Cartesian coordinates. This radial quantity, S is defined as:

$$s = \begin{Bmatrix} d + \frac{R(\cos - \cos)}{\cos\cos} - \left(R\tan\beta(\frac{\phi}{\tan\beta} - z_{m,n} + P(1 - \frac{\theta_{m,n}}{2\pi})\tan\beta R)\right)\phi^{-1} \\ d + \tan\alpha\left(-\frac{\phi}{\tan\beta} - z_{m,n} + P(1 - \frac{\theta_{m,n}}{2\pi})\right) \\ d - Rr - \sqrt{R^2 - \left(z_{m,n} - P(1 - \frac{\theta_{m,n}}{2\pi})\right)^2} \end{Bmatrix} \quad (12)$$

Where, φ= Rr + (R/cosα). Converting these radial quantities into Cartesian coordinates results in:

$$x_{p_{m,n}} = s\cos\theta_{m,n}, \quad y_{p_{m,n}} = s\sin\theta_{m,n}, \quad z_{p_{m,n}} = z_{m_{m,n}} = z_{i_{m,n}} \quad (13)$$

VI. Experimental validation

Flow forming is typically applied to forming metallic components involving high speeds, feed rates and forming forces. Due to the nature of the process, it is difficult to completely stop the process at a particular point in time in a safe manner such that the instantaneous forming zone is preserved. Therefore, the forming speeds, forces and feed rates must be significantly reduced in order to study the tooling/workpiece interaction in flow forming. In order to validate the analytical model above, a physical model of flow forming was developed using Plasticine conforming to ASTMD-4236. The suitability of using Plasticine and similar compounds to model metal forming processes has been established by Sofuoglu and Rasty(2000) as well as Pertence and Cetlin (1998). All material preparation steps detailed by Sofuoglu and Rasty (2000) were followed. The contact condition used for validation was designed to provide geometry that other modeling efforts have failed to address. Specifically, the contact of a nosed roller with a nose/nose entry condition of type 'AII'. Unlike the other contact conditions, this type is the most complex in terms of curvature as there is no straight/linear section appearing anywhere on

the surface. The tooling used was a smooth mandrel with Rm = 69.33mm and a roller with Rr = 56.23mm, R = 5.00mm, α=45o and β=60o. These were installed on a lathe with a thread-cutting feed set such that P = 2.54 mm/rev. The mandrel was dusted with talcum powder and Plasticine of a uniform thickness to= 8.05mm was set on it. The outer surface of the Plasticine was also dusted with talcum powder. The roller was brought into contact with the Plasticine such that tf = 6.17 with n = 5rev/min. The steel and Plasticine process components were all measured with standard contact measurement apparatus with an accuracy of ±0.01mm. This reduction level was selected such that it maximized the size of the contact patch with the given tooling and minimized bulging of material ahead of the roller. Despite these precautions, there was some build-up of material ahead of the roller. The forming was stopped with a brake after two full rotations of the mandrel resulting in the contact patch of the roller mid-forming. [5-12]

Figs. 3 and 4 show the 2D plots of the analytical profile of the roller in relation to corresponding nearest neighbor experimental points on the xy plane (Fig. 3) and the zx plane (Fig. 4). These two plots show the proximity of the analytical surface to the experiment alone. Outside of the area influence of the roller, there is a lack of coherence with the analytical surface. This is due to the inherent bulging of material ahead of the roller both axially and tangentially. Also they show that the peak distance, approximately 0.35mm, occurs along the axial entry profile due to the minor bulging of material as it encounters the roller. However, there is very little change in the circumferential δDi gradient despite the overall surface variation which re-asserts the accuracy of the fit. [5-12]

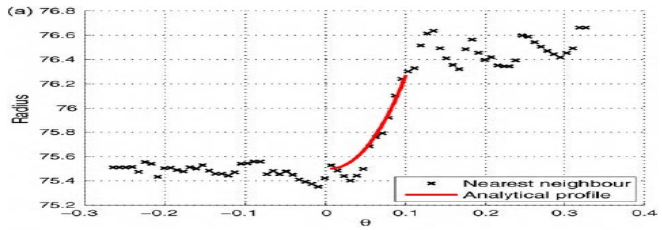

(a)

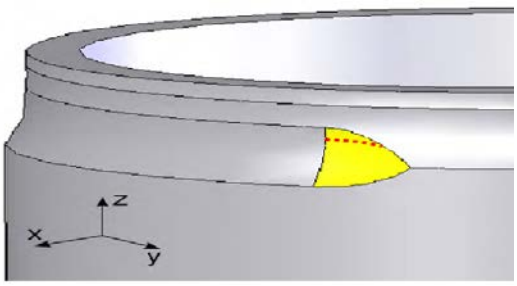

(b)

Fig.3. Analytical profile of the roller in the best-fit position with the corresponding nearest neighbour experimental points on the (a) xy plane and (b) the location of these points on the relevant portion of the surface in 3D.

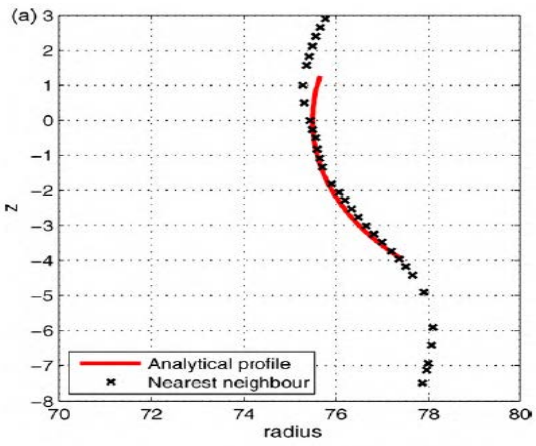

(a)

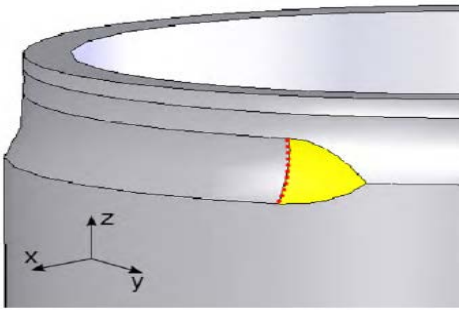

(b)

Fig.4. Analytical profile of the roller in the best-fit position with the corresponding nearest neighbour experimental points on the (a) zx plane and (b) the location of these points on the relevant portion of the surface in 3D

VII. CONCLUSION

An analytical model of the roller/workpiece interface in flow forming has been developed such that it may predict the contact area. This model is applicable to all tooling geometries for both forward and backward flow forming processes. Due to the general nature of the description of the geometry, the approach taken can be used for other rotary forming operations where a die or a roller is used to deform a cylindrical workpiece locally. This model has been compared to experimental data generated from physical modeling and shows excellent correspondence. Specifically, the analytical model was found to describe the experimental surface within 0.4mm based on MSE.

The independent geometric variables examined were starting and final thicknesses (t0, tf), forming pitch (P), mandrel radius (Rm), attack angle (α) as well as roller and roller nose radii (Rr, R). These variables were modified over a range of 125% for the starting thickness and 150% for all others. Specific findings showed that on the basis of a unit change in the respective variables:

• t0 had four times the effect on the change in overall area and components

• tf had 33% more of an effect

• P had 50% less of an effect, with the exception of the tangential deformation component, Axy which had 50% more of an effect

• Rm, ، , and Rr have less than a 27% effect
• R caused the least change: less than 7% change in area

The present work could be extended to study the multi-variant effects on the contact area to fully account for the geometric changes during complicated forming processes. However, geometric factors are not the only process parameters which govern the process. The main direction of future work is to link the geometric factors to other process factors such as workpiece material properties and tribological considerations to gain deeper insight into the overall process mechanics.

ACKNOWLEDGMENT

Islamic Azad University, Neyriz Branch supported this work. We would like to thank this university.

REFERENCES

[1] M. Gur, J. Tirosh, Plastic flow instability under compressive loading during shear spinning process, Transactions of the ASME, Journal of Engineering for Industry 104 (1982) 17–22.
[2] P.R. Singhal, P.K. Saxena, R. Prakash, Estimation of power in the shear spinning of long tubes in hard-to-work materials, Journal of Materials Processing Technology 23 (1990) 29–40.
[3] K. Xue, Z. Wang, Y. Lu, K. Li, Elasto plastic FEM analysis and experimental study of diametral growth in tube spinning, Journal of Materials Processing Technology 69 (1997) 172–175.
[4] Y. Xu, S.H. Zhang, P. Li, K. Yang, D.B. Shan, Y. Lu, 3D rigidplastic FEM numerical simulation of tube spinning, Journal of Materials Processing Technology 113 (2001) 710–713.
[5] M. J. Roy, D. M. Maijer, R. J. Klassen, J. T. Wood, E. Schost, Analytical solution of the tooling/workpiece contact interface shape during a flow forming operation', Journal of Materials Processing Technology 210, 14 (2010) 1976-1985.
[6] K. Li, N. Hao, Y. Lu, K. Xue, Research on the distribution of the displacement in backward tube spinning, Journal of Materials Processing Technology 79 (1998) 185–188.
[7] K. Xue, Y. Lu, X. Zhao, A study of matching relationships amongst technical parameters in stagger spinning, Journal of Materials Processing Technology 69 (1997) 167–171.
[8] K. Xue, Y. Lu, X. Zhao, The disposal of key problems in the FEM analysis of tube stagger spinning, Journal of Materials Processing Technology 69 (1997) 176–179.
[9] T.R. Mohan, R. Misra, Studies on power spinning of tubes, International Journal of Production Research 10 (1970) 351–364.
[10] M. Hayama, H. Kudo, Analysis of diametrical growth and working forces in tube spinning, Bulletin of Japan Society of Mechanical Engineers 22 (1979) 776–784.
[11] T. Wang, Z.R. Wang, Q. Wang, Y. Zhao, S. Wang, The slipline fields of thickness-reduction spinning and the engineering calculation of the spinning forces, in: Proceedings of the Fourth International Conference of Rotary Forming, October, 135–139, 1989, pp. 89–93.
[12] J.-W. Park, Y.-H. Kim, W.-B. Bae, Analysis of tube spinning processes by the upper bound stream function method, Journal of Materials Processing Technology 66 (1997) 195–203.

Hamidreza Gharehchahi was born in Isfahan, Iran in 26 April 1977. He graduated from Tabriz University on Mechanical Engineering in 2000, Tabriz, Iran. Then he passed the M.Sc. program at Iran University of Science and Technology on Mechanical Engineering in 2003, Tehran, Iran. Most of the time, he was very active at class and he got top marks in some courses.
He has held positions on the Mechanical Engineering Department of the Islamic Azad University and he was the head of Mechanical Engineering Department for one year at Neyriz Branch. Now, he is a Full time faculty member and student deputy of Neyriz Branch, Islamic Azad University, Neyriz, Iran. His major fields of study are Manufacturing, CAD/CAM, Metal Forming, and Advanced Manufacturing Technology.

Mr. Gharehchahi is member of *International Association of Computer Science and Information Technology*, *Science and Engineering Institute (SCIEI)* of USA, IAS (Iran Aerospace Society) and *Society Manufacturing Engineering* of Iran. He issues 15 papers in different journals and conferences. He was Top Researcher of Islamic Azad University, Neyriz Branch in 2011.

Amin Etminan was born in 1 September 1982 in Shiraz. He graduated from Persian Gulf University on Fluid Mechanics in 2004. Then he passed the M.Sc. course at Yazd University on Fluid Mechanics/Energy Conversion in 2007. Most of the time, he was very active at class and got top marks in some courses. He participated in some regional, national and international conferences on Mechanical Engineering and related fields. However, his major field of study is turbulent fluid flow, heat transfer and stress analysis.

He has held positions on the Mechanical Engineering Department of the Islamic Azad University as senior lecturer and he was the head of Mechanical Engineering Department for two years at Neyriz Branch. In addition, to some research papers, he authored; "Determination of Flow Configurations and Fluid Forces Acting on two Tandem Square Cylinders in Cross-Flow and its Wake Patterns," International Journal of Mechanics, USA, 2010, "Instantaneous and Time-Averaged Flow Structure around two Heated Square Cylinders in the Laminar Flow Regime," Applied Mechanics and Materials Journal, Switzerland, 2012, "Exergy Analysis of Micro Gas Turbine Tri-Generation System," Advanced Materials Research Journal, Switzerland, 2012. He succeed to earn top author awards in some international conference.

Mr. Etminan is an official licensee member of *Iranian Engineering Organization in Construction Activities*, *International Association of Computer Science and Information Technology (IACSIT)*, *Science and Engineering Institute (SCEI)* and *International Scientific Academy of Engineering & Technology (ISAET)*. He was Top Researcher of Islamic Azad University, Neyriz Branch in 2011 and 2012.